

## **SUPPLEMENTAL ITEM 1**

### **Bulk trace element partition coefficients estimated from pumice-glass pairs**

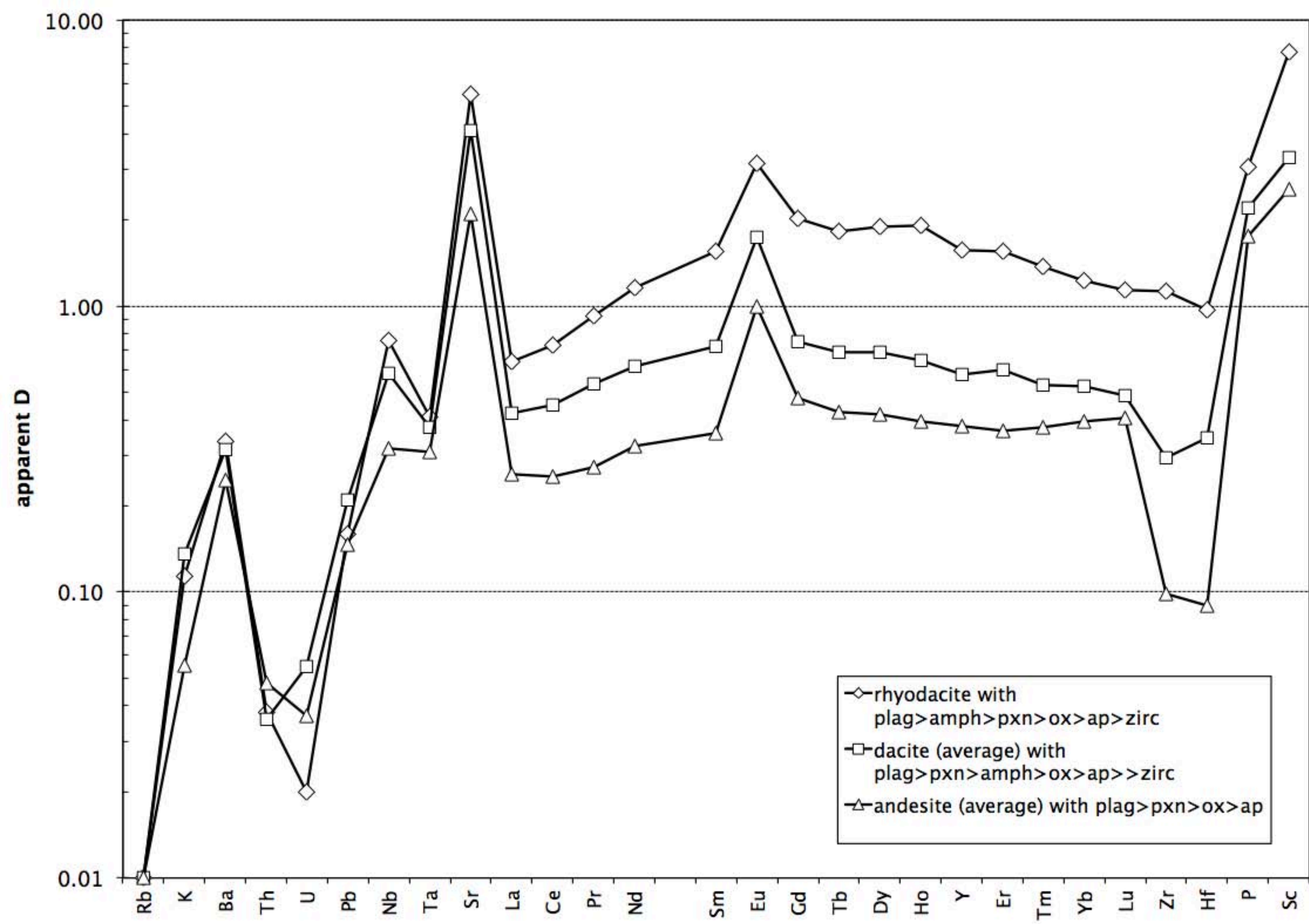
Effective bulk partition coefficients can be obtained from pumice-glass pairs if the pumice whole-rock compositions are adjusted for their glass fractions to derive the trace element concentrations of the bulk crystal assemblages. Glass fractions were not separated quantitatively and weighed, nor point-counted, but can be estimated by assigning a suitably low bulk partition coefficient for an incompatible element, and then calculating glass and crystal fractions by mass-balance. Numerically removing this fraction of glass from the pumice analysis, then renormalizing, yields an estimate of the trace element concentrations of the bulk crystal assemblage. The pumices lack a K-rich mineral, so Rb is here assigned a bulk D (mineral assemblage/melt) of 0.01. Table DR1 and figure DR1 present effective bulk partition coefficients for pyroxene andesites (average of 2), amphibole-pyroxene dacites (average of 2), and the amphibole rhyodacite. Effective Ds for most elements increase systematically as the melts become more evolved, as amphibole replaces pyroxenes as the dominant mafic silicate, as zircon joins the crystal assemblage, and (presumably) as magmatic temperature decreased. The systematic nature of the changes is evidence that crystal growth from melt dominates the element enrichments and depletions, although the rocks contain complexly zoned crystals, probably due to more diverse processes.

## **SUPPLEMENTAL ITEM 2**

### **Modeling of crystal fractionation effects on oxygen isotopes**

Progressive crystal fractionation will generally increase the  $\delta^{18}\text{O}$  values of successively more evolved magmas, but the magnitude of increase varies with crystallizing phase assemblage,

proportions, and temperature (Eiler, 2001; Bindeman et al., 2004). Probable crystallizing phase proportions for Mount Rainier were determined by calculating average magma compositions for  $\text{SiO}_2$  intervals for the whole-rock suite, and relating these averages by least-squares multiple regression involving representative plagioclase, hypersthene, augite, titanomagnetite, ilmenite, and apatite compositions (Stockstill et al., 2002; Sisson and Vallance, 2009; Sisson, unpublished). Mineral-melt oxygen isotope fractionation factors were then estimated by two methods, and the crystallizing phase assemblages were stepwise fractionated in increments of 1 wt% of remaining melt to derive oxygen isotope evolution with magmatic differentiation. The two models for oxygen isotope fractionation factors were (1) the melt wt%  $\text{SiO}_2$ -based approximations for plagioclase and pyroxene of Bindeman et al. (2004), and (2) mineral-pair fractionation factors summarized by Chacko et al. (2001), including the estimated difference between orthopyroxene and clinopyroxene shown by Eiler (2001), and assuming that ilmenite fractionates oxygen isotopes equivalent to magnetite. This second approach treats the melt as an equivalent CIPW normative mineral assemblage to calculate phenocryst-melt fractionation, and assumes that temperature and plagioclase anorthite content decrease linearly with increasing melt  $\text{SiO}_2$  (1100 to 750 °C and  $\text{An}_{70}$  to  $\text{An}_{25}$  for 55 to 75 wt%  $\text{SiO}_2$ ). The two approaches yield similar results, with  $\delta^{18}\text{O}$  of the melt increasing at 0.04 to 0.05 ‰ per wt%  $\text{SiO}_2$  (Figure 6), moderately steeper than fractionation trajectories estimated for differentiation of arc magmas in Kamchatka (0.01-0.02 ‰ per wt%  $\text{SiO}_2$ ) based on thermodynamic simulations of crystallization-differentiation (Bindeman et al., 2004).



[illegible]

| rock type                 | Rb*  | K    | Ba   | Th   | U    | Pb   | Nb   | Ta   | Sr  | La   | Ce   | Pr   | Nd   | Sm   | Eu   | Gd   | Tb   | Dy   | Tm   | Ho   | Y    | Er   | Yb   | Lu   | Zr   | Hf   | P   | Sc  |
|---------------------------|------|------|------|------|------|------|------|------|-----|------|------|------|------|------|------|------|------|------|------|------|------|------|------|------|------|------|-----|-----|
| rhyodacite (01GPM1)       | 0.01 | 0.11 | 0.34 | 0.04 | 0.02 | 0.16 | 0.76 | 0.41 | 5.5 | 0.64 | 0.73 | 0.92 | 1.16 | 1.55 | 3.15 | 2.02 | 1.81 | 1.89 | 1.90 | 1.56 | 1.56 | 1.37 | 1.23 | 1.14 | 1.12 | 0.97 | 3.1 | 7.7 |
| dacites (05K1921-1 & -2)  | 0.01 | 0.14 | 0.31 | 0.04 | 0.06 | 0.21 | 0.58 | 0.38 | 4.1 | 0.42 | 0.45 | 0.53 | 0.62 | 0.72 | 1.73 | 0.75 | 0.69 | 0.69 | 0.64 | 0.58 | 0.60 | 0.53 | 0.52 | 0.49 | 0.29 | 0.35 | 2.2 | 3.3 |
| andesites (08RE1034A & I) | 0.01 | 0.06 | 0.25 | 0.05 | 0.04 | 0.15 | 0.32 | 0.31 | 2.1 | 0.26 | 0.25 | 0.27 | 0.32 | 0.36 | 0.99 | 0.47 | 0.43 | 0.42 | 0.39 | 0.38 | 0.37 | 0.38 | 0.40 | 0.41 | 0.10 | 0.09 | 1.8 | 2.6 |

dacite and andesite values are averages of two named samples; \* Rb assigned value of 0.01 to derive glass fractions